

# Chapter 22

## Monitoring Land Use and Land Cover Analysis of the Barak Basin Using Geospatial Techniques



Wajahat Annayat , Kumar Ashwini, and Briti Sundar Sil 

### 22.1 Introduction

Human beings need land for their survival and development (Xie et al., 2020). Land is becoming a scarce resource due to human-induced environmental changes such as expansion of agriculture, logging of forests, road hydropower and urbanization and setup of new mining industries (Ellwanger et al., 2020). Both natural and anthropogenic factors and their utilization by humans with space and time are responsible for the change in pattern of LULC of a particular region (Ganaie et al., 2020). From global to local scale, it has been widely accepted that LULC plays an important role on the functioning of the ecosystem. LULC of every continent has been comprehensively modified since the development of agriculture (Saunders et al., 1991). The nature of this modification is both dynamic and nonlinear which are activated by various factors such as social, political, economic and environmental factors which lead to the change in the climate (Reid et al., 2000; Webb & Honda, 2007; Miyamoto et al., 2014; Hassan et al., 2016). The process of LULC is not simple, as because there are structural complexities between various types of LULC changes which are changing both in space and time (Lambin et al., 2003).

All over the world, various researchers have investigated the analysis of changes in the LULC. Monitoring of LULC should be conducted on regular basis as because it causes various irreversible influences on the environment, particularly causing urban micro-climate warming (Coppin et al., 2004; Hahs et al., 2009; Niyogi et al., 2010; Wajahat & Sundar, 2018; Policelli et al., 2018). Satellite images of different spectral, spatial and temporal resolution have been used to carry out a LULC mapping successfully (Friedl et al., 2010; Solaimani et al., 2010; Aredehey et al., 2018). Monitoring and planning of LULC changes in the arid and semiarid regions, and the use of satellite images has been less used (Jia et al., 2014; Aredehey et al.,

---

W. Annayat (✉) · K. Ashwini · B. S. Sil  
Department of Civil Engineering, National Institute of Technology, Silchar, Assam, India

2018; Teka et al., 2018). In order to utilize the natural resources with proper planning and management, the study of LULC is mandatory. Traditional methods for collecting data are not sufficient to study the multi-complex environmental studies (Deng et al., 2009), since a lot of difficulties persists in order to present the multidisciplinary data set. In order to detect the changes in the LULC, accurate and timely data of various land utilizations of an area are required (Bastawesy et al., 2008). Hence, we require technologies like remote sensing (RS) and geographical information systems (GIS) to present these data sets. These technologies provide data at those places where field investigations are rare and difficult to attain.

Series of 30 years of data has been used to study the LULC changes in the Barak River which are based on RS and GIS technology. In the literature, authors found that in the Barak River till date, no study has been carried out which is based on the temporal and spatial channel changes in the LULC. So in order to fulfil this gap and to understand the nature and causes of LULC change in the Barak Basin, it is further planned to carry out a study through which the proper dynamics of the LULC changes of the Barak River can be understood. In this work, we have presented the changes in the LULC with the help of Landsat data by using a classification known as hybrid classification which consists of both supervised classification and unsupervised classification. The main aim of the present work is to apply RS and GIS techniques in order to understand temporal and spatial channel changes of LULC with a long period of time (1988–2018). In order to fulfil the main aim of the study, the following objectives are framed to carry out this study in the Barak River which is outlined below:

- To delineate the various LULC patterns
- To analyse the various changes in LULC categories from 1988 to 2018

The outcome of the study on the monitoring land use and land cover analysis of the Barak Basin using geospatial techniques is subdivided into seven sections. Following this introduction represents a synthesis of the relevant literature on river LULC analysis. Section 22.2 deals with the description of the study area highlighting the location and climatic peculiarities. Section 22.3 illustrates the materials and methods and data used and discusses the methodologies. Sections 22.4 narrate the results and discussion of the spatio-temporal variability of LULC. Section 22.5 summarizes the results and provides the major conclusions from the present study. The final section consists of reference section which is included at the end.

## 22.2 Study Area

The total length of Barak River is 900 km long and is flowing through the various states such as Manipur, Nagaland, Mizoram and Assam in India and into the Bay of Bengal via Bangladesh. In Bangladesh, this river is known by a name called as Surma River. From 900 km, 524 km is in India, and the rest is in Bangladesh. In the northeast India, Barak River is the second largest river which is flowing parallel to

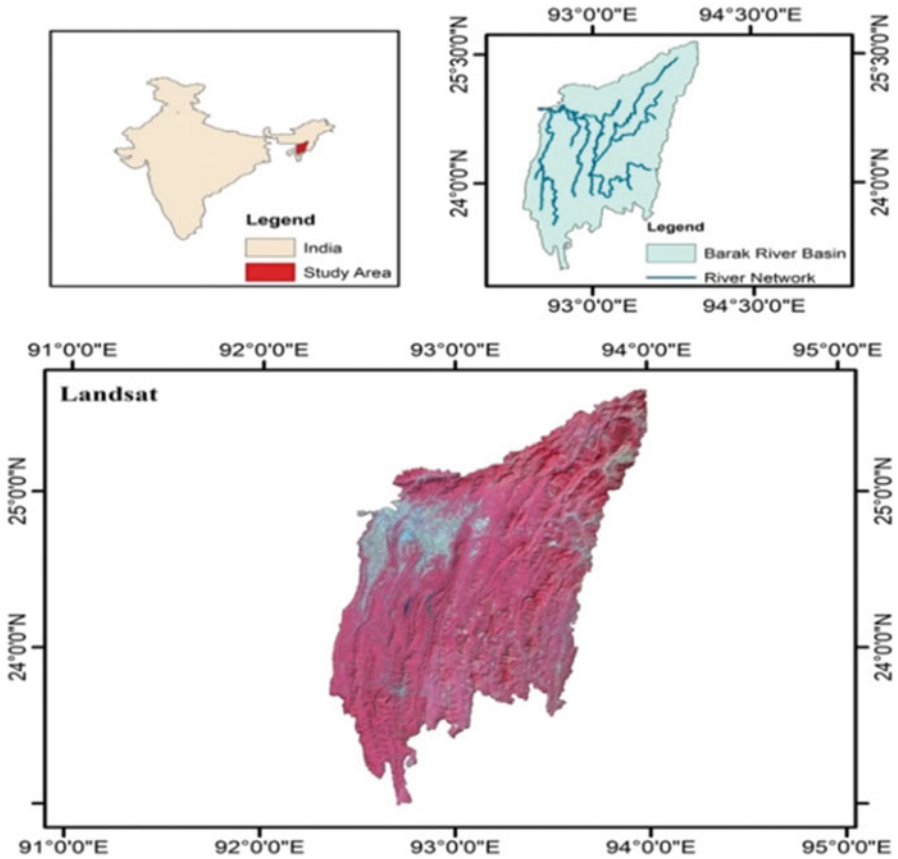


**Fig. 22.1** Location of the study area

the river Brahmaputra. Barak River starts from the Manipur hills of the Japvo Mountain .The Barak Basin lies between 90°50'E to 95°0'E and 22°43'N to 25°57'N. It was found that the annual rainfall varies from 2500 to 4000 mm out of which 80% of the annual rainfall has occurred in the monsoon season (April to October) (Annayat & Sil, 2020a). The mean annual  $T_{min}$  and  $T_{max}$  ranged from 17.74 to 19.617 °C and 25.147 to 29.652 °C, respectively (Annayat & Sil, 2020b). In this study, analysis of LULC has been conducted for the whole of the Barak Basin located in India covering a distance of approximately 524 km. The location map of the study area is shown in Fig. 22.1.

## 22.3 Materials and Methods

### 22.3.1 Data Used

Basic data used in this study include multi-date Landsat images of the years 1988 (MSS), 1998 (MSS), 2008 (TM) and 2018 (OLI). In this study, four-time series satellite images were obtained from the United States Geological Survey (USGS). All the five satellite raw images were attained on separate years, i.e. 1988 (MSS), 1998 (MSS), 2008 (TM) and 2018 (OLI). The detailed information of Landsat images used is shown in Table 22.1. Also we have shown satellite raw images based on their capturing time (Fig. 22.2).

### 22.3.2 Methodology

After downloading the Landsat data, Landsat 1 (MSS) was subjected to line destripping (line stripping was found) as scanning error was removed by the filtering techniques (Pan & Chang, 1992). The resolution of Landsat 1(MSS) was 60 m; we georeferenced the data by using various control points in order to improve the positional accuracy and to resample the MSS data into 30 m resolution. Also ERDAS IMAGINE 14 software was used to carry out the radiometric error and haze corrections (Hazarika et al., 2015; Annayat & Sil, 2021). A combined method of classification (supervised and unsupervised) was used to classify the LULC (Hazarika et al., 2015). Through supervised classification, we assign the signature file of different classes by visual interpretation. Accordingly, the data is reclassified into eight classes, namely, water bodies, vegetation and dense vegetation, agricultural land, built-up, grassland, wasteland and riverbed (Aboelnour & Engel, 2018). We assess the classified data in order to find its accuracy by using a matrix known as confusion matrix (Abdelkareem et al., 2017). We compare the values of error in each class, which were classified one-to-one value in the ground truth data. A total of 240 ground truth points were used for the accuracy assessment. Same number of columns and rows were possessed by the table which is equal to the number of classes. The present chart of the methodology shows the schematic flow diagram of the whole work (Fig. 22.3).

A significant step in the classification of images is the accuracy assessment. From the error matrix, some of the processes of accuracy assessment are kappa coefficient

**Table 22.1** Dataset utilized in the study

Data type	Sensor	Path/row	Scale	Acquisition date	Source
Landsat 1	MSS	136/43	60 m	05.01.1988	
Landsat 2	MSS	136/43	30 m	09.12.1998	<a href="http://earthexplorer.usgs.gov">http://earthexplorer.usgs.gov</a>
Landsat 5	TM	136/43	30 m	04.02.2008	
Landsat 8	OLI	136/43	30m	20.12.2018	

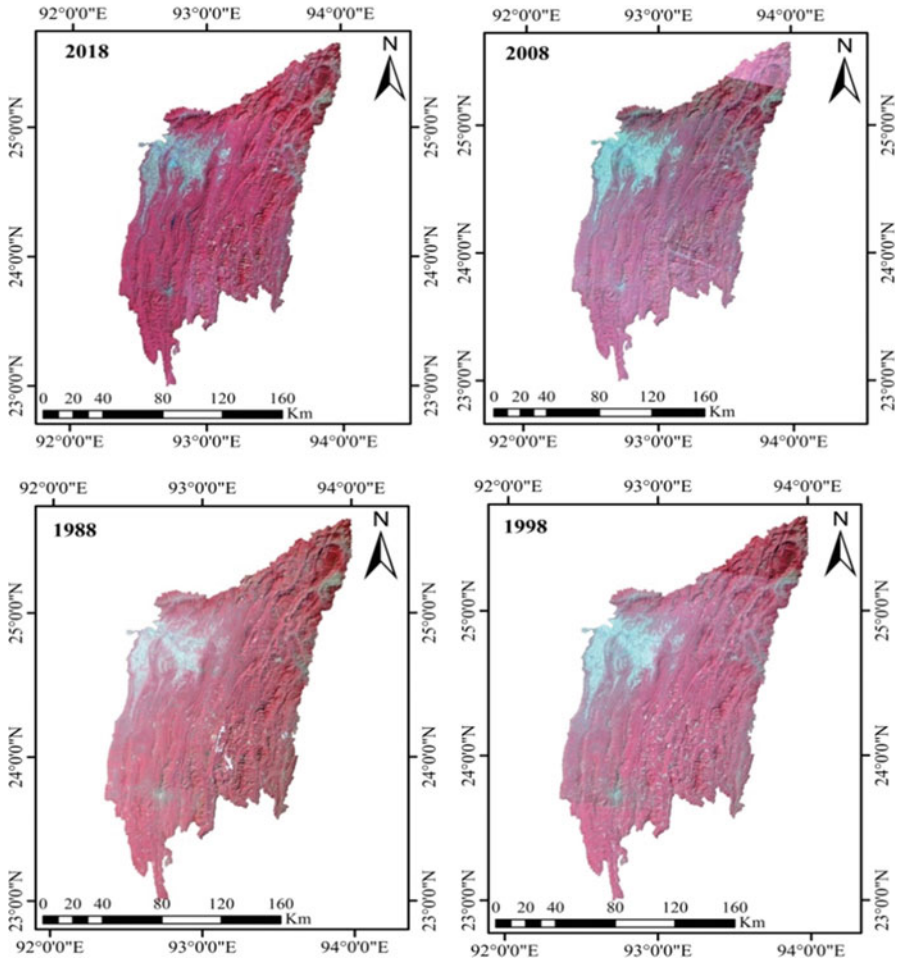


**Fig. 22.2** Satellite raw images based on their capturing time

( $K^{\wedge}$ ), overall accuracy, producer’s accuracy and user accuracy (Zhang et al., 2016). Then the kappa coefficient ( $K^{\wedge}$ ) is then calculated using the following equation (Abdelkareem et al., 2017).

$$K = \frac{N \sum_{i=1}^r X_{ii} - \sum_{i=1}^r X_{i+} X_{+i}}{N^2 - \sum_{i=1}^r X_{i+} X_{+i}} \tag{22.1}$$

where

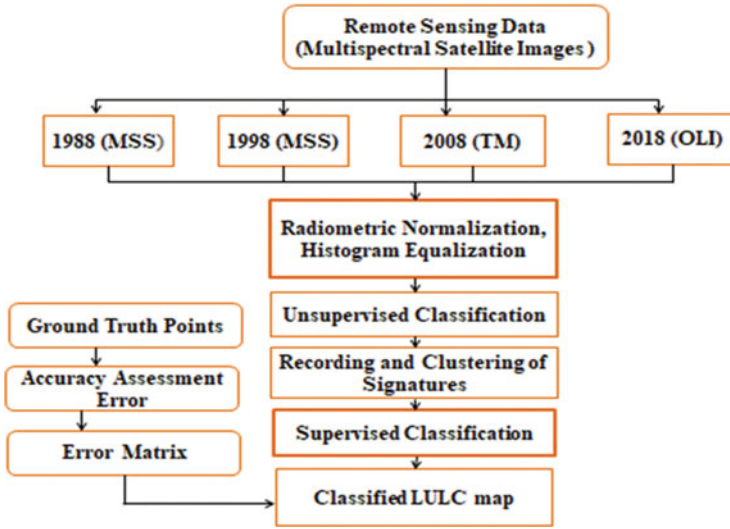


Fig. 22.3 Flow chart for methodology

- r = “Number of rows/columns in confusion matrix”
- X<sub>ii</sub> = “Number of observation in row i and column i”
- X<sub>i+</sub> = “Total number of row i”
- X<sub>+i</sub> = “Total number of column i”
- N = “Number of observations”

Percentage of samples which are correctly classified in an error matrix is known as classification accuracy. In order to calculate the classification accuracy, we divide the total number of samples which are correctly classified by the total number of reference samples. It can be expressed by the following equation (Dada & Hahn, 2020):

$$\text{Overall accuracy} = \frac{\text{“Number of Sampling classes classified correctly”}}{\text{“Number of reference sampling classes”}} \quad (22.2)$$

In order to derive the mapping accuracy of LULC classes, both producers accuracy and user accuracy are calculated using the Eqs. 22.3 and 22.4 (Story & Congalton, 1986) and (Congalton & Green, 2019).

$$\text{Producers accuracy} = \frac{a_{ii}}{\sum_{i=1}^n a_{i+}} \quad (22.3)$$

$$\text{User accuracy} = \frac{a_{ii}}{\sum_{i=1}^n a_{+i}} \quad (22.4)$$

where

$a_{ii}$  = “Number of samples correctly classified”

$a_{i+}$  = “Column total for class i”

$a_{+i}$  = “Row total for class i”

## 22.4 Results and Discussion

### 22.4.1 Land Use Classification

In order to analyse the LULC changes at different times, it gives an idea about the probable driving factors which are responsible for the level of changes and its consequences. Also respective management techniques are utilized in order to prevent the further loss of LULC in a particular area. The analysis of the entire land use and land cover of the study area in 1988, 1998, 2008 and 2018, respectively, reflected different proportions of changes that occurred in water bodies, vegetation and dense vegetation, agricultural land, built-up, grassland, wasteland and riverbed. Table 22.2 and Fig. 22.4 give the statistical results of LULC changes. Evaluation of LULC was done between 1988 and 2018. Changes were evaluated from the differences between 1988 and 1998, 1998 and 2008, 2008 and 2018 and 1988 and 2018. Eight major LULC types such as water bodies, vegetation, dense vegetation, agricultural land, built-up, grassland, wasteland and riverbed were registered and considered for the study area. In order, the abundance of different categories of LULC till 1988 are represented as dense vegetation (76.59)> vegetation (14.04)> agricultural land (5.23)> water (1.88)>urban and built-up area (1.49)> grassland (0.486)> wasteland (0.1)> riverbed (0.087), while as for the year 2018, the situation was somehow different and can be represented as dense vegetation (74.02)> vegetation (15.37)> agricultural land (5.69)> urban and built-up area (2.59)> water (1.44) > grassland (0.55)> riverbed (0.20)> and wasteland (0.10). During the recent years, significant momentum has been gained by the studies of the LULC on the environment and the society. LULC changes that are derived from the period of 30 years

**Table 22.2** Land use/land cover changes of the Barak River Basin from 1988 to 2018

Area coverage				
LULC Class	1988	1998	2008	2018
Water	458.14	392.85	518.53	350.58
Vegetation	3407.12	3848.27	3934.42	3730.67
Dense vegetation	18584.95	18120.98	17811.47	17960.69
Agricultural	1270.63	1298.41	1254.86	1382.41
Urban/built-up	361.68	432.24	562.81	628.48
Grassland	118.99	108.40	131.24	134.61
Wasteland	40.17	44.69	14.20	25.73
Riverbed	21.16	17.02	35.31	49.66
Total	24262.87	24262.87	24262.87	24262.87

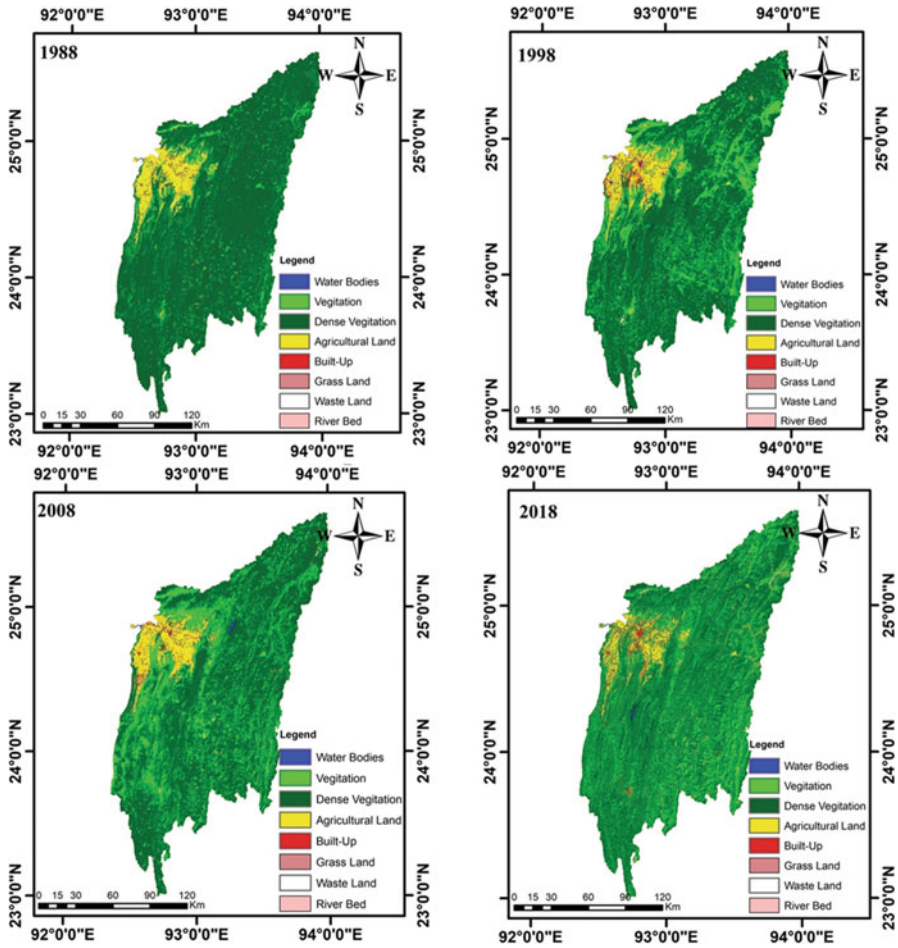


**Fig. 22.4** Land use/land cover changes for three decades (1988–2018) in the Barak River Basin

(1988–2018) have been shown in Table 22.3 and Fig. 22.4. It is evident from Table 22.3 that the LULC changes were of highest amount in riverbed and urban from 1988 to 2018. Dominant land use that increased progressively over the study period was urban, grassland and agricultural land. For example, urban increased by 19.50% for 1988–1998, 30.20% for 1998–2008 and 73.76% for 1988–2018, while agricultural land increased by 2.18% for 1988–1998, 10.16% for 2008–2018 and 8.08% for 1998–2018. In addition, grassland increased by 21.06% and 13.12% from 1998 to 2008 and 1988 to 2018, respectively. In contrast, water decreased by 14.2% for 1988–1998 and 32.39% for 2008–2018 and 23.48% for 1988–2018. Dense vegetation showed a decreasing trend by 2.49% for 1988–1998, 1.70% for 1998–2008 and 3.48% for 1988–2018. Wasteland showed a decreasing trend of 35.92% for 1988–2018. Rapid population growth, migration of rural people to



**Table 22.3** Change of LULC class through change matrix from 1988 to 2018

Class	1988-1998		1998-2008		2008-2018		1988-2018	
	Change in area in km <sup>2</sup>	% Change*	Change in area in km <sup>2</sup>	% Change*	Change in area in km <sup>2</sup>	% Change*	Change in area in km <sup>2</sup>	% Change*
Water	-65.29	-14.24	125.68	31.99	-167.95	-32.39	-107.56	-23.48
Vegetation	441.15	12.94	86.15	2.23	-203.75	-5.17	323.55	9.5
Dense vegetation	-463.97	-2.49	-309.51	-1.7	149.22	0.83	-624.26	-3.48
Agricultural	27.78	2.18	-43.55	-3.35	127.55	10.16	111.78	8.08
Urban/built-up	70.56	19.5	130.57	30.2	65.67	11.66	266.8	73.76
Grassland	-10.59	-8.89	22.84	21.06	3.37	2.57	15.62	13.12
Wasteland	4.52	11.27	-30.49	-68.22	11.53	81.24	-14.44	-35.92
Riverbed	-4.14	-19.57	18.29	107.44	14.35	40.63	28.5	134.62

\*Cover change between periods is calculated as  $\left( \frac{B_{Final Year} - B_{Initial Year}}{B_{Initial Year}} \right) * 100$ , where B = area of LULC

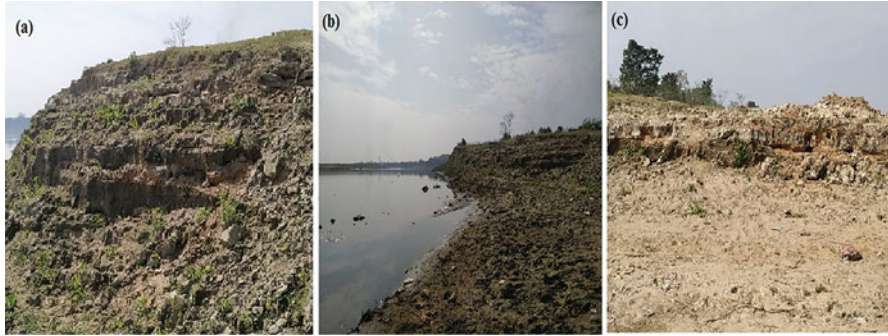


**Fig. 22.5** Field photo of LULC of the Barak River at various locations: (a) Fulertal (b) Anapurna (c) Badarpur

urban, unawareness of biophysical limitations and poverty are some of the probable reasons behind the changes in the LULC. In addition to industrial, agricultural and other activities, humans also affect climate through changes in land use (activities taking place on land, like growing food, cutting trees, or building cities) and land cover (the physical characteristics of the land surface, including grain crops, trees or concrete). Some field photographs (Fig. 22.5) show the LULC of the Barak River. From Table 22.3, it is clear that the change in area under urban and built-up was 19.5% during 1988–1998, while this change in area was 73.76% during 1988–2018. It is clear that the area under urban and built-up has increased; besides, this erosion of bank tries to capture the area which is nearby the settlement.

#### 22.4.2 Overall Classification Accuracy and Kappa Statistics

It is very difficult to assess the classification accuracy as it is associated with lot of problems (Foody, 2002). Overall accuracy is one of the basic accuracy measures, and it is obtained by dividing the properly classified pixels by the total number of pixels (Banko, 1998). A statistical valid assessment for the quality of classification is provided by kappa coefficient, and it is a measure of overall agreement of matrix. All the diagonal elements are taken into consideration in case of kappa coefficient (Rosenfield & Fitzpatrick-Lins, 1986). The results of the hybrid classification of the LULC of the Barak River for the Landsat 1 (1988; MSS), Landsat 2 (1998; MSS), Landsat 5 (2008; TM) and Landsat 8 (2018; OLI) showed overall classification accuracy of 93.75%, 92.96%, 95.42% and 97.50% with overall kappa statistics of 0.9283, 0.9183, 0.9476 and 0.9714, respectively (Table 22.4). Some other studies have observed similar range of results such as in Umabdalla Natural Reserved Forest, South Kordofan, Sudan by Abdelkareem et al. (2017) and in Lodhran District of Pakistan by Hussain et al. (2019). As per (Pontius Jr (2000), the value of kappa coefficient greater than 0.5 is considered as satisfactory for modelling of LULC changes. However, Landis and Koch (1977) set a range of kappa coefficient as

**Table 22.4** Overall classification and kappa statistics of the Barak River Basin using hybrid classification

Accuracy	Barak River			
	1988	1998	2008	2018
Overall classification accuracy (%)	93.75	92.96	95.42	97.50
Kappa statistics (K)	0.9283	0.9183	0.9476	0.9714

follows: a value of kappa coefficient greater than 0.7 is considered as excellent, values between 0.6 and 0.79 are considered as substantial and values of 0.59 or less indicate moderate or poor agreement. The overall accuracy and kappa coefficient of the present study are within the excellent range.

Concerning the overall producer and user accuracy for the classified imagery classes from 1988 to 2018, the result revealed excellent user accuracy for nearly all the classes in all years (Table 22.4). From all the classified images, water and agricultural land are the best classified with almost 100% accuracy as because of distinctive separation from the rest of the classes. For water, the best accuracy was obtained in the year 1998 where both producer and user accuracy are 100%. Similarly for agricultural land, the best accuracy was obtained in the year 2018 where both producer and user accuracy are 100%. Finally from Table 22.5, overall classification accuracies such as producer accuracy and user accuracy suggested that this classification is consistent and satisfactory for further analysis.

## 22.5 Conclusion

The Barak River is the second largest river in the northeast India. Main incentive of this chapter is to analyse the changes in the LULC of the Barak River using the remote sensing data and GIS technology. Four different Landsat images were used in order to under the dynamics of the LULC changes. The findings of the present study reveal that the LULC changes were significant from 1988 to 2018. It was found that water, dense vegetation and wastelands area have decreased by 23.48%, 3.48% and 35.92%, respectively, in 2018. However, agricultural, grassland, urban and riverbed have increased by 8.08%, 13.12%, 73.76 and 134.62%, respectively, which clearly indicate that there is a major impact of humans and their developmental activities on the LULC changes. The overall accuracy such as producer accuracy, user accuracy and kappa coefficient of the present study are within the excellent range.

**Table 22.5** Summary of producer and user accuracy assessment for supervised classification of land use land cover in the Barak River during the years (1988, 1998, 2008 and 2018)

Year	1988			2008			2018		
	Producers accuracy	Users accuracy	Producers accuracy	Users accuracy	Producers accuracy	Users accuracy	Producers accuracy	Users accuracy	
Water	96.77%	100.00%	100.00%	100.00%	93.55%	96.67%	100.00%	90.00%	
Vegetation	93.33%	93.33%	90.32%	93.33%	100.00%	86.67%	100.00%	100.00%	
Dense vegetation	93.33%	93.33%	96.55%	93.33%	88.24%	100.00%	90.91%	100.00%	
Agricultural	93.75%	100.00%	100.00%	93.33%	100.00%	96.67%	100.00%	100.00%	
Urban/built-up	90.00%	90.00%	79.41%	90.00%	93.55%	96.67%	100.00%	95.00%	
Grassland	100.00%	90.00%	89.66%	86.67%	96.77%	100.00%	95.24%	100.00%	
Wasteland	96.43%	90.00%	100.00%	93.33%	96.55%	93.33%	100.00%	95.00%	
Riverbed	81.25%	92.86%	75.00%	100.00%	96.55%	93.33%	95.24%	100.00%	

**Acknowledgements** ‘We are thankful to USGS, for providing us data, and other support for completion of this work’.

**Disclosure Statement** ‘The authors reported no potential conflict of interest’.

## References

- Abdelkareem, O. E. A., Elamin, H. M. A., Eltahir, M. E. S., Adam, H. E., Elhaja, M. E., Rahamtalla, A. M., Babatunde, O., & Elmar, C. (2017). Accuracy assessment of land use land cover in Umabdalla Natural Reserved Forest, South Kordofan, Sudan. *International Journal of Agricultural and Environmental Sciences*, 3(1), 5–9.
- Aboelnour, M., & Engel, B. A. (2018). Application of remote sensing techniques and geographic information systems to analyze land surface temperature in response to land use/land cover change in Greater Cairo Region, Egypt. *Journal of Geographic Information System*, 10(1), 57–88.
- Annayat, W., & Sil, B. S. (2020a). Assessing channel morphology and prediction of centerline channel migration of the Barak River using geospatial techniques. *Bulletin of Engineering Geology and the Environment*, 1–23.
- Annayat, W., & Sil, B. S. (2020b). Changes in morphometric Meander parameters and prediction of Meander channel migration for the alluvial part of the Barak River. *Journal of the Geological Society of India*, 96(3), 279–291.
- Annayat, W., & Sil, B. S. (2021). Predicting Meander migration of the Barak river by empirical and time sequence methods. *Water Security and Sustainability: Proceedings of Down To Earth*, 2019, 113.
- Aredehey, G., Mezgebu, A., & Girma, A. (2018). Land-use land-cover classification analysis of Giba catchment using hyper temporal MODIS NDVI satellite images. *International Journal of Remote Sensing*, 39(3), 810–821.
- Banko, G. (1998). *A review of assessing the accuracy of classifications of remotely sensed data and of methods including remote sensing data in forest inventory*.
- Bastawesy, M. A., Khalaf, F. I., & Arafat, S. M. (2008). The use of remote sensing and GIS for the estimation of water loss from Tushka lakes, southwestern desert, Egypt. *Journal of African Earth Sciences*, 52(3), 73–80.
- Congalton, R. G., & Green, K. (2019). *Assessing the accuracy of remotely sensed data: Principles and practices*. CRC press.
- Coppin, P., Jonckheere, I., Nackaerts, K., Muys, B., & Lambin, E. (2004). Review Article Digital change detection methods in ecosystem monitoring: A review. *International Journal of Remote Sensing*, 25(9), 1565–1596.
- Dada, E., & Hahn, M. (2020). Application of satellite remote sensing to observe and analyse temporal changes of cocoa plantation in Ondo State, Nigeria. *GeoJournal*, 1–16.
- Deng, J. S., Wang, K., Hong, Y., & Qi, J. G. (2009). Spatio-temporal dynamics and evolution of land use change and landscape pattern in response to rapid urbanization. *Landscape and Urban Planning*, 92(3–4), 187–198.
- Ellwanger, J. H., Kulmann-Leal, B., Kaminski, V. L., Valverde-Villegas, J., Veiga, A. N. A. B. G., Spilki, F. R., Fearnside, P. M., Caesar, L., Giatti, L. L., & Wallau, G. L. (2020). Beyond diversity loss and climate change: Impacts of Amazon deforestation on infectious diseases and public health. *Anais da Academia Brasileira de Ciências*, 92(1).
- Foody, G. M. (2002). Status of land cover classification accuracy assessment. *Remote Sensing of Environment*, 80(1), 185–201.

- Friedl, M. A., Sulla-Menashe, D., Tan, B., Schneider, A., Ramankutty, N., Sibley, A., & Huang, X. (2010). MODIS Collection 5 global land cover: Algorithm refinements and characterization of new datasets. *Remote Sensing of Environment*, *114*(1), 168–182.
- Ganaie, T. A., Jamal, S., & Ahmad, W. S. (2020). Changing land use/land cover patterns and growing human population in Wular catchment of Kashmir Valley, India. *GeoJournal*, 1–18.
- Hahs, A. K., McDonnell, M. J., McCarthy, M. A., Vesk, P. A., Corlett, R. T., Norton, B. A., Clemants, S. E., Duncan, R. P., Thompson, K., & Schwartz, M. W. (2009). A global synthesis of plant extinction rates in urban areas. *Ecology Letters*, *12*(11), 1165–1173.
- Hassan, Z., Shabbir, R., Ahmad, S. S., Malik, A. H., Aziz, N., Butt, A., & Erum, S. (2016). Dynamics of land use and land cover change (LULCC) using geospatial techniques: A case study of Islamabad Pakistan. *Springerplus*, *5*(1), 812.
- Hazarika, N., Das, A. K., & Borah, S. B. (2015). Assessing land-use changes driven by river dynamics in chronically flood affected Upper Brahmaputra plains, India, using RS-GIS techniques. *The Egyptian Journal of Remote Sensing and Space Science*, *18*(1), 107–118.
- Hussain, S., Mubeen, M., Ahmad, A., Akram, W., Hammad, H. M., Ali, M., Masood, N., Amin, A., Farid, H. U., & Sultana, S. R. (2019). Using GIS tools to detect the land use/land cover changes during forty years in Lodhran District of Pakistan. *Environmental Science and Pollution Research*, 1–17.
- Jia, K., Liang, S., Wei, X., Yao, Y., Su, Y., Jiang, B., & Wang, X. (2014). Land cover classification of Landsat data with phenological features extracted from time series MODIS NDVI data. *Remote Sensing*, *6*(11), 11518–11532.
- Lambin, E. F., Geist, H. J., & Lepers, E. (2003). Dynamics of land-use and land-cover change in tropical regions. *Annual Review of Environment and Resources*, *28*(1), 205–241.
- Landis, J. R., & Koch, G. G. (1977). An application of hierarchical kappa-type statistics in the assessment of majority agreement among multiple observers. *Biometrics*, 363–374.
- Miyamoto, M., Parid, M. M., Aini, Z. N., & Michinaka, T. (2014). Proximate and underlying causes of forest cover change in Peninsular Malaysia. *Forest Policy and Economics*, *44*, 18–25.
- Niyogi, D., Kishtawal, C., Tripathi, S., & Govindaraju, R. S. (2010). Observational evidence that agricultural intensification and land use change may be reducing the Indian summer monsoon rainfall. *Water Resources Research*, *46*(3).
- Pan, J.-J., & Chang, C.-I. (1992). Destriping of Landsat MSS images by filtering techniques. *Photogrammetric Engineering and Remote Sensing*, *58*, 1417.
- Policelli, F., Hubbard, A., Jung, H. C., Zaitchik, B., & Ichoku, C. (2018). Lake Chad total surface water area as derived from land surface temperature and radar remote sensing data. *Remote Sensing*, *10*(2), 252.
- Pontius, R. G., Jr. (2000). Comparison of categorical maps. *Photogrammetric Engineering and Remote Sensing*, *66*, 1011–1016.
- Reid, R. S., Kruska, R. L., Muthui, N., Taye, A., Wotton, S., Wilson, C. J., & Mulatu, W. (2000). Land-use and land-cover dynamics in response to changes in climatic, biological and socio-political forces: the case of southwestern Ethiopia. *Landscape Ecology*, *15*(4), 339–355.
- Rosenfield, G. H., & Fitzpatrick-Lins, K. (1986). A coefficient of agreement as a measure of thematic classification accuracy. *Photogrammetric Engineering and Remote Sensing*, *52*(2), 223–227.
- Saunders, D. A., Hobbs, R. J., & Margules, C. R. (1991). Biological consequences of ecosystem fragmentation: A review. *Conservation Biology*, *5*(1), 18–32.
- Solaimani, K., Arekhi, M., Tamartash, R., & Miryaghobzadeh, M. (2010). Land use/cover change detection based on remote sensing data (A case study; Neka Basin). *Agriculture and Biology Journal of North America*, *1*(6), 1148–1157.
- Story, M., & Congalton, R. G. (1986). Accuracy assessment: A user's perspective. *Photogrammetric Engineering and Remote Sensing*, *52*(3), 397–399.
- Teka, H., Madakadze, C. I., Botai, J. O., Hassen, A., Angassa, A., & Mesfin, Y. (2018). Evaluation of land use land cover changes using remote sensing Landsat images and pastoralists

- perceptions on range cover changes in Borana rangelands, Southern Ethiopia. *International Journal of Biodiversity and Conservation*, 10(1), 1–11.
- Wajahat, A., & Sundar, S. B. (2018). Estimation and analysis of possible flood for the Silchar city-a case study. *Disaster Advances*, 11(1).
- Webb, E. L., & Honda, K. (2007). Biophysical and policy drivers of landscape change in a central Vietnamese district. *Environmental Conservation*, 164–172.
- Xie, H., Zhang, Y., Wu, Z., & Lv, T. (2020). A bibliometric analysis on land degradation: Current status, development, and future directions. *Land*, 9(1), 28.
- Zhang, Z., Liu, S., Wei, J., Xu, J., Guo, W., Bao, W., & Jiang, Z. (2016). Mass change of glaciers in Muztag Ata–Kongur Tagh, Eastern Pamir, China from 1971/76 to 2013/14 as derived from remote sensing data. *PLoS One*, 11(1), e0147327.